

Study of the chemical evolution and spectral signatures of some interstellar precursor molecules of adenine, glycine & alanine

Liton Majumdar^a, Ankan Das^a, Sandip K. Chakrabarti^{b,a}, Sonali Chakrabarti^{c,a}

^aIndian Centre For Space Physics, 43 Chalantika, Garia Station Road, Kolkata 700084, India

^bS.N. Bose National Center for Basic Sciences, JD-Block, Salt Lake, Kolkata, 700098, India

^cMaharaja Manindra Chandra College, 20 Ramakanto Bose Street, Kolkata, 700003, India

Abstract

We carry out a quantum chemical calculation to obtain the infrared and electronic absorption spectra of several complex molecules of the interstellar medium (ISM). These molecules are the precursors of adenine, glycine & alanine. They could be produced in the gas phase as well as in the ice phase. We carried out a hydro-chemical simulation to predict the abundances of these species in the gas as well as in the ice phase. Gas and grains are assumed to be interacting through the accretion of various species from the gas phase on to the grain surface and desorption (thermal evaporation and photo-evaporation) from the grain surface to the gas phase. Depending on the physical properties of the cloud, the calculated abundances varies. The influence of ice on vibrational frequencies of different pre-biotic molecules was obtained using Polarizable Continuum Model (PCM) model with the integral equation formalism variant (IEFPCM) as default SCRF method with a dielectric constant of 78.5. Time dependent density functional theory (TDDFT) is used to study the electronic absorption spectrum of complex molecules which are biologically important such as, formamide and precursors of adenine, alanine and glycine. We notice a significant difference between the

spectra of the gas and ice phase (water ice). The ice could be mixed instead of simple water ice. We have varied the ice composition to find out the effects of solvent on the spectrum. We expect that our study could set the guidelines for observing the precursor of some bio-molecules in the interstellar space.

Keywords: Molecular clouds, Interstellar medium, chemical evolution, Star formation

1. Introduction

Presence of interstellar dust towards the formation of complex interstellar molecules is taken for granted especially after the discovery of more than twenty molecules around the star forming region in the interstellar ice. Altogether, according to the CDMS catalog (<http://www.astro.uni-koeln.de/cdms/molecules>), one hundred and seventy molecules have been detected in the interstellar medium or circumstellar shells. To model the formation of complex molecules, and especially through interstellar grain chemistry, several attempts were made by various workers (Chakrabarti et al., 2006ab; Das et al., 2008b; Das, Acharyya & Chakrabarti 2010; Cuppen et al., 2007; Cuppen et al., 2009 etc.) over the years. Interstellar dust grains are thought to be consisting of amorphous silicate or carbonaceous core surrounded by molecular ice layer (Draine et al., 2003; Gibb et al., 2004). It has been clear from the experimental and observational results that almost 90% of the grain mantle is covered with H₂O, CH₃OH, CO₂ (Keane et al., 2001, Das et al., 2011 and references therein). Presence of HCN, CN, CS and H₂O in space were identified by anomalous absorption (Omont 1993 & Bujarrabal et

Email addresses: liton@csp.res.in (Liton Majumdar), ankan.das@gmail.com (Ankan Das), chakraba@bose.res.in (Sandip K. Chakrabarti), sonali@csp.res.in (Sonali Chakrabarti)

al., 1994). But a complete understanding of the chemical and physical processes which take place on a grain surface is still missing.

The origin of amino acids through the pre-biotic chemistry of the early earth has been a topic of long standing interest. However, complex pre-biotic molecules might also be formed due to very complex and rich chemical processes inside a molecular cloud. The production of amino acids, nucleobases, carbohydrates and other basic compounds can possibly start from the molecules like HCN, cyano compounds, aldehyde, and ketones (Orgel 2004; Abelson 1966), which could lead to the origin of life in the primitive earth conditions. However, even with the present observational tools, it is hard to confirm the presence of any bio-molecules in the ISM. So it may suffice, if we can identify a few precursor molecules which eventually form bio-molecules in the interstellar space. Quantum chemical simulations could be used to find out the spectral properties of these complex molecules. It is observed and experimentally verified that the spectral signature of a species significantly deviates between the gas phase and the ice phase. So a theoretical study of the spectral properties of the precursors of some important bio-molecules in both the gas and ice phases could serve as benchmarks for the observations.

In this Paper, we consider a large gas-grain network coupled with a hydrodynamic simulation to obtain the abundances of various complex molecules, which could lead to the formations of adenine, alanine & glycine. We also discuss the production of formamide which is an important precursor in the process of the abiotic synthesis of amino acids. In the literature, there are several observational studies on glycine (Kuan et al., 2003, Hollis et al. 2003, Snyder et al. 2005, etc.). But its existence in a molecular

cloud, till date, is not verified without a reasonable doubt. In case of adenine, we find that though its abundance in our theoretical model is well under the observation limit, its precursor molecules are heavily abundant. It is also true for the alanine and glycine. These prompted us to find out the spectral signatures of the precursor molecules of these three molecules around the different astrophysical environment, from which one could roughly anticipate the abundances of adenine, glycine & alanine. All possible reaction pathways are included in the gas as well as in the grain phase network. Armed with the chemical abundances of these precursor molecules, we compute the infrared and electronic absorption spectra in the gas as well as for the icy grains.

The plan of this paper is the following. In Section 2, the models used and the computational details are presented. Implications of the results are discussed in Section 3. Finally, in Section 4, we draw our conclusions.

2. Computational details

2.1. Hydro-chemical Model

The process of formation of complex molecules in the interstellar space is very much uncertain. There could be a number of pathways available for the formation of a complex molecule. However, depending on the chemical abundances of the reactive species and the reaction cross section, the rate of formation varies. Formation routes of several interstellar bio-molecules are already reported in Majumdar et al., (2012). They pointed out that despite of the huge abundances of the neutral species, radical-molecular/radical-radical reaction pathways dominates towards the formation of some pre-biotic species. Normally such reactions are barrier less and exothermic in nature.

To study the chemical evolution of various complex radicals, ions, molecules which are very much important for the prebiotic synthesis of different bases of amino acids, we have constructed a hydro-chemical model to mimic the interstellar scenario.

The evolution of the chemical species is strongly dependent on the physical properties of the medium. So the dynamic nature of the medium at any particular instant could influence the chemical composition of the medium. Das et al., (2008b) & Das et al., (2010) considered a spherically symmetric isothermal (10K) collapsing cloud, whose outer boundary was assumed to be located at one parsec and the inner boundary was assume to be located at 10^{-4} parsec. They used a finite difference Eulerian scheme (upwind scheme) to solve the Eulerian equations of hydrodynamics in spherical polar coordinates. Since they were interested in the spherical case, they only considered radial motion and ignored any dependency upon the θ & ϕ coordinates. By solving the hydrodynamic equations they studied fully time-dependent behaviour of the spherical flow.

To have a realistic condition, we have considered this density distribution as an input for our chemical model. The gas phase chemical network is mainly adopted from the UMIST 2006 database (Woodall et al., 2007). Here, we have chosen the initial elemental abundances according to the Woodall et al., (2007), these are the typical low-metal abundances often adopted for TMC-1 cloud. We add a few new reactions following Chakrabarti et al., (2000ab), Woon et al., (2002), Quan & Herbst (2007), Gupta et al., (2011) and references therein. Recently, Majumdar et al., (2012), calculated the rate coefficients for the reaction pathways described in Chakrabarti et al., 2000ab. They used Bates (1983) semi-empirical formula to find out the rate coefficients

of any chemical reactions. Gupta et al.(2011) also followed the same prescription to find out the reaction rates for the adenine formation in interstellar space.

To show the importance of grains towards the chemical enrichment of the ISM, we have also included a detailed grain chemistry network following Hasegawa, Herbst & Leung (1992), Das et al., (2008a), Das et al., (2010), Cuppen et al., (2007), Jones et al., (2011), Garrod et al., (2008) and Das & Chakrabarti (2011) into our reaction network. We therefore have the most updated chemical network to study the chemical evolution of several interstellar species. In order to perform a self-consistent study, we assume that the gas and the grains are coupled through the accretion and the thermal evaporation processes. We assume that the species are physisorbed onto the dust grain (classical size grain $\sim 1000 \text{ \AA}$) having the grain number density $1.33 \times 10^{-12}n$, where n is the concentration of H nuclei in all forms. Thus, in principle, we have a complete interstellar model, which could be used to follow the hydro-chemical properties of a collapsing cloud.

2.2. *Quantum chemical calculation*

First of all, we have optimized the geometry of the molecules, which are the precursors of various bio-molecules in space. In order to have an idea for the stability of these molecules, B3LYP/6-311++G** level is used. Gas phase vibrational frequencies of these precursor molecules are also calculated by the B3LYP/6-311++G** level.

Observational evidences suggest that grain mantles around the dense clouds are mainly covered by H₂O (> 60%), CH₃OH (2-30% with respect to solid water) and CO₂ (2-20 % with respect to solid water). To find out the effects of the solvent on the spectrum, we have chosen three types of ice. (i) Unless otherwise stated,

we use pure water ice. (ii) We use methanol ice also to mimic the ice composition around the methanol rich environment and finally, (iii) Based on the observational results, we construct an ice, which consists of 70% water 20% methanol and 10% carbon-di oxide and call is as the ‘mixed ice’.

In order to find out the vibrational frequencies of these molecules in the ice phase, we have optimized the geometry of these molecules in ice at B3LYP/6-311++G** level. Here, the Polarizable Continuum Model (PCM) model is used with the integral equation formalism variant (IEFPCM) as the default SCRF method. We have chosen IEFPCM model as a convenient one, since the second energy derivative is available for this model and also it is analytic in nature. Vibrational frequencies given here are not exactly for the ice phase since the dielectric constant of ice (85.5) is slightly higher than that of water (78.5). We have calculated also the electronic absorption spectrum of these molecules using the time dependent density functional theory (TDDFT study).

3. Result and Discussion

Till date, due to the constraints on the observational sensitivity, it is quite challenging to directly identify interstellar bio-molecules. For instance, the observational report on glycine by Kuan et al., (2003) was not supported by Hollis et al. (2003) and Snyder et al. (2005). Chemical models (Chakrabarti & Chakrabarti 2000ab, Das et al., 2008b, Majumdar et al., 2012) predict that the trace amount of bio-molecules could be produced during the collapsing phase of a proto-star. Since the abundances of these molecules are very low, it is possible that they are not directly observable with the present day technology. However, if we concentrate on the pathways through which

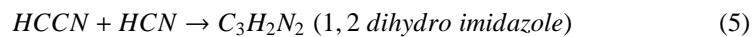
these molecules form in the ISM and identify the precursor molecules, it could be much easier to predict their abundances. This is what is done in our work. We compute their chemical abundances after considering the gas-grain interaction in our chemical model and present the spectral signatures of the precursor molecules in the gas phase as well as in the grain phase. Water is found to be the most abundant molecule followed by Methanol and Carbon-di-oxide in the ice phase. We have concentrated on the changes of the spectral signature between the gas phase and ice phase. The spectral changes with the changes of solvents are also highlighted.

3.1. Precursor molecules of adenine

There are a few studies related to the formation of adenine. Chakrabarti et al., (2000ab) proposed a neutral-neutral pathways for the formation of adenine. According to them, the adenine could be produced by the following reactions:



Recently Gupta et al. (2011) proposed that the following radical-molecular reaction network, which could lead to the adenine formation.



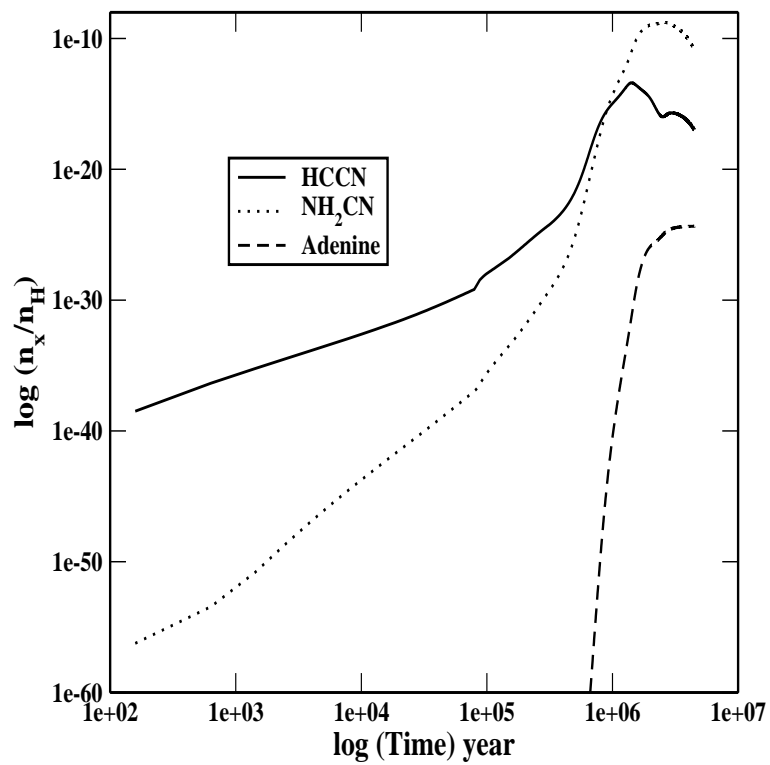
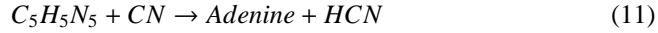
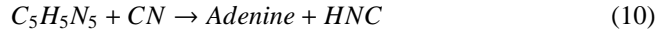
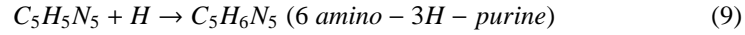
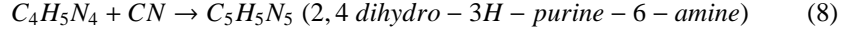
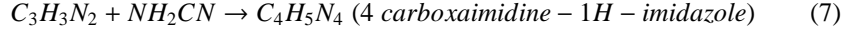
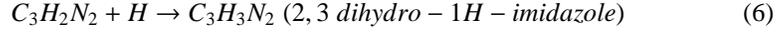


Figure 1: Time evolution of adenine with its two precursor molecules. Since the precursors are several orders of magnitude higher, the probability of their detection is higher.



In the chemical model described in Majumdar et al. (2012), the reactions 1 to 11 were included and it was concluded that the production of adenine is dominated by the radical-molecular reaction pathways. HCCN and NH₂CN are the two important molecules, which are responsible for the production of adenine by the radical-molecular pathways. So we could treat HCCN and NH₂CN as the precursor molecules for the production of interstellar Adenine. HCCN is highly abundant in the interstellar space (Jiurys et al., 2006, Guelin & Cernicharo 1991). The formation of HCCN on the grain was considered by Hasegawa, Herbst & Leung (1992). McGonagle & Irvine (1996) conducted a deep search for HCCN towards TMC-1 and several GMC's via its N(J)=1(2)→0(1) transition. They set an upper limit of fractional abundance with respect to molecular hydrogen of 2×10^{-10} . The existence of NH₂CN in the interstellar cloud was first reported by Turner et al. (1975). After that it was observed in both diffuse and dense clouds by Liszt & Lucas (2001). Woodall (2007) predicted a steady state fractional abundance of 2.02×10^{-10} for NH₂CN with respect to H₂.

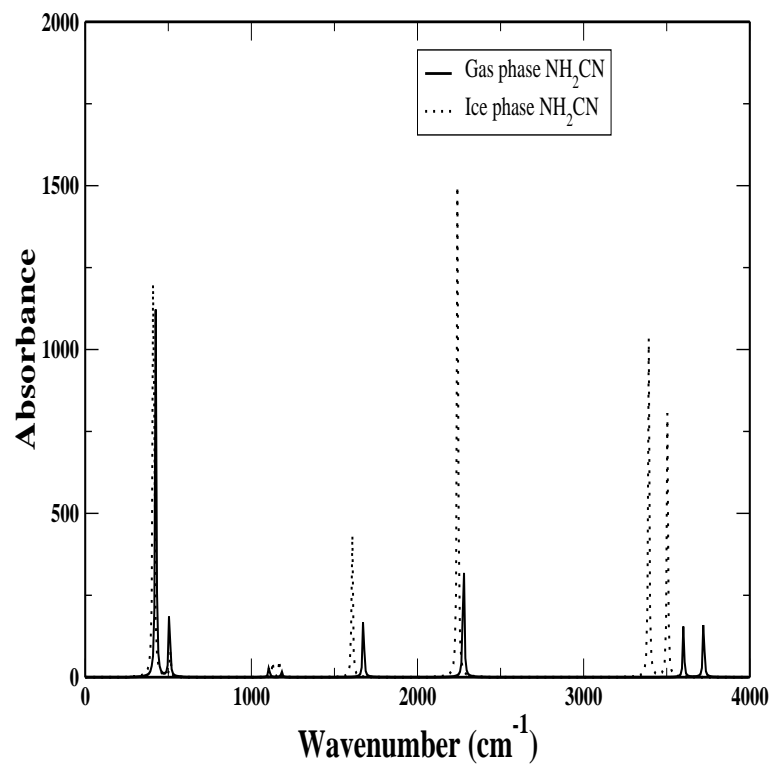


Figure 2: Infrared spectrum of NH_2CN in gas as well as in H_2O ice. The line strength in the ice phase is generally several times higher.

We already mentioned that we are using the density distribution of our hydrodynamical model as an input of our chemical model. Since production of complex species in the intermediate region of the cloud is favourable, we consider the density distribution of intermediate region as an input of our chemical model. In Fig. 1, we present the chemical evolution of adenine in gas phase along with its two precursor molecules, namely, HCCN & NH₂CN. We find that the abundance of NH₂CN is significantly higher, having a peak abundance of 1.7×10^{-9} and a final abundance of NH₂CN (after $\sim 5 \times 10^6$ years) is 1.38×10^{-11} with respect to total hydrogen nuclei. **In our case, final abundance of NH₂CN appears to be slightly lower than the amount calculated by Woodall et al., (2007). This is probably because Woodall et al., (2007) carried out their simulation by assuming a constant density cloud (10^4 cm^{-3}), whereas in our case, we consider a realistic density distribution obtained from the isothermal hydrodynamic model. Moreover, our chemical network consists of a large gas-grain network whereas the grain-surface network is missing in Woodall et al., (2007).** Peak value of the HCCN abundance is found to be 4.1×10^{-14} and finally it turns out to be 1.14×10^{-17} . With these two significantly abundant molecules, adenine could be produced with an abundance of 4.4×10^{-25} . In our hydrodynamic model, density around the inner grid locations started to increase rapidly after 10^5 years. The reason behind this is that after one dynamical time scale (\sim free fall time $\sim 10^5$ years), there are the smooth transport of matter from the outer envelope to the inner envelope. After some dynamical times (i.e., around 10^6 years), core mass gets heavier and induce more matter from the cloud than the matter actually accreting to the cloud through the outer envelope. Finally, the cloud relaxes to a steady state density distribution. Since there

was a sharp rise in density between 10^5 - 10^6 years for our hydrodynamical model, our chemical evolution also shows (Fig. 1) sharp rise in the abundances during that period. Since we chose the initial elemental abundances following Woodall et al. (2007), basically, we started with zero abundance of any complex species.

NH_2CN is a planar pentatomic molecule. It has nine fundamental vibrations (Rubalcava, 1956). In Fig. 2, infrared absorption spectra of NH_2CN for the gas phase and ice phase is shown. We note that the gas phase NH_2CN has its strongest feature at 424 cm^{-1} and the second intense peak arises at 2277 cm^{-1} . In the ice phase 424 cm^{-1} peak is shifted to the left and appear at 411 cm^{-1} and peak at 2277 cm^{-1} is also shifted in the left and appear at 2241 cm^{-1} with much higher intensity. Rubalcava (1956) assigned a vibrational peak for the gas phase NH_2CN at 2275 cm^{-1} which was shifted at 2257 cm^{-1} in the solution of methylene chloride at 25°C . Beside these intense peaks there are several peaks which are pronounced in our ice phase model (such as peaks at 3391 cm^{-1} and 3504 cm^{-1}). For the sake of better understanding, we tabulate all the infrared peak positions with their absorbance in Table 1. In Table 1, we note down the peak position of the infrared spectrum of cyanocarbene (HCCN) in the gas as well as in the ice phase. We find that the most intense mode in the gas phase appears at 3442 cm^{-1} . This peak is shifted in the left in the ice phase by 186 cm^{-1} and appears at 3256 cm^{-1} . Other peaks in the gas phase have negligible contributions. One weak peak at 1261 cm^{-1} appears in the ice phase. McCarthy et al. (1995) detected rotational transitions from seven low-lying vibrational states of HCCN with a sensitive millimeter-wave spectrometer. They obtained a peak at 3256 cm^{-1} , which is exactly coinciding with our strongest peak at the ice phase. Dendramis and Leroi (1977) performed a matrix isolation spec-

Table 1: Vibrational frequencies of different complex molecules in gas phase, H₂O ice and methanol containing grains at B3LYP/6-311G++** level

Species	Peak positions (Gas phase) (Wavenumber in cm ⁻¹)	Absorbance	Peak positions (H ₂ O ice) (Wavenumber in cm ⁻¹)	Absorbance	Peak positions (Methanol ice) (Wavenumber in cm ⁻¹)	Absorbance
HCCN	361.81	0.02	365.76	.001	365.66	0.002
	472.51	0.48	476.23	1.84	476.15	1.78
	953.94	2.43	962.29	3.9	962.2	3.85
	1264.15	3.11	1261.21	20.78	1261.32	19.79
	1837.77	1.67	1842.18	.33	1842	0.36
	3442.74	72.88	3256.78	296.99	3264.26	285.76
NH ₂ CN	399.44	1.18	411.2	558.25	411.91	549.69
	424.58	331.27	419.28	0.64	418.19	1.36
	506.79	78.52	511.60	21.81	511.20	23.53
	1106.5	11.24	1129.17	14.95	1128.48	14.9
	1182.24	5.81	1167.57	15.23	1168.24	14.82
	1674.56	68.34	1606.43	144.79	1609.51	141.85
	2277.03	142.76	2241.40	486.82	2242.75	471.1
	3601.35	49.83	3391.73	300.21	3400.13	287.59
	3722.54	64.62	3504.14	232.97	3512.95	225.09
CH ₂ NH ₂	318.67	500.63	395.86	381.58	399.5	392.74
	906.57	7.79	454.78	36.29	433.45	36.96
	1247.51	43.21	484.98	287.53	496.42	262.89
	1295.04	9.11	927.74	5.58	929.13	5.2
	1488.33	0.03	1232.40	54.84	1233.35	54.55
	1697.65	61.9	1305.44	11.38	1306.49	11.11
	3175.48	11.04	1482.85	2.88	1484.23	2.92
	3302.9	13.91	1658.80	105.1	1660.7	103.69
	3618.37	18.34	3121.60	19.78	3120.02	19.94
	3744.57	20.4	3244.2	22.13	3241.7	22.41
	-	-	3454.87	83.77	3463.3	79.24
	-	-	3574.02	87.41	3582.74	83.04
COOH	563.02	174.43	527.91	274.95	525.87	270.55
	564.06	37.16	576.96	88.35	576.21	85.09
	971.71	185.63	1004.45	360.38	1005.32	353.26
	1246.79	2.28	1238.63	12.42	1242.43	11.59
	1719.72	337.79	1661.63	634.66	1663.93	619.87
	3427.26	1.56	2759.29	339.39	2808.53	311.42
C ₂ H ₃ ON	93.80	73.46	227.10	24.35	219.98	24.79
	227.28	12.91	236.09	21.97	235.28	21.72
	654.85	5.11	659.67	12.28	659.02	11.85
	679.23	105.13	698.25	142.52	696.02	141.02
	933.22	9.24	932.94	1.37	932.81	1.33
	1133	357.05	1086.56	948.30	1086.95	923.82
	1187.76	184.8	1187.07	176.63	1187.21	178.39
	1453.73	1.06	1443.51	4.87	1443.04	4.98
	1476.31	0.67	1484.93	0.19	1484.08	0.16
	2127.17	299.17	2131.47	734.61	2133.49	720.19
	3229.69	2.38	3205.66	1.28	3209.03	1.32
	3384.87	7.47	3365.84	11.18	3369.44	11
	3505.82	84.71	3474.5	180.74	3479.12	177.75
C ₃ H ₅ ON	191.8	3.32	191.32	15.01	194.43	10.05
	218.57	21.96	222.92	3.13	224.96	4.01
	267.93	27.05	263.17	186.82	265.86	78.55
	290.27	130.59	278.65	134.51	298.21	198.11
	387.79	19.01	392.16	18.82	394.74	19.99
	570.49	11.56	573.19	6.55	573.64	7.09
	584.91	4.19	596.31	2.59	596.93	2.57
	788.74	16.30	802.39	8.91	893.81	80.95
	902.23	31.88	894.69	79.43	1032.76	89.02
	1033.80	83.20	1031.17	108.92	1089.89	11.37
	1094.69	10.61	1085.35	12.45	1137.77	44.92
	1135.26	47.07	1133.81	48.79	1273.41	22.11
	1278.81	10.48	1260.6	63.62	1373.41	22.11
	1356.76	3.7	1363.86	18.47	1390.68	5.87
	1400.34	23.91	1378.94	11.81	1447.1	13.89
	1449.81	9.51	1443.03	12.52	1509.23	13.09
	1523.18	10.39	1509.64	11.54	1520.34	10.94
	1526.22	7.22	1521.19	9.31	2272	11.98
	2277.03	0.9	2270.35	19.92	3042.14	13.61
	3027.25	10.75	2972.02	2.17	3048.99	9.08
	3079.31	0.37	3032.65	11.22	3122.11	22.68
	3104.22	22.68	3112.9	16.33	3130.03	23.59
	3121.81	13.86	3121.92	16.47	3659.5	46.27
	3646.01	20.12	3243.97	248.16	-	-

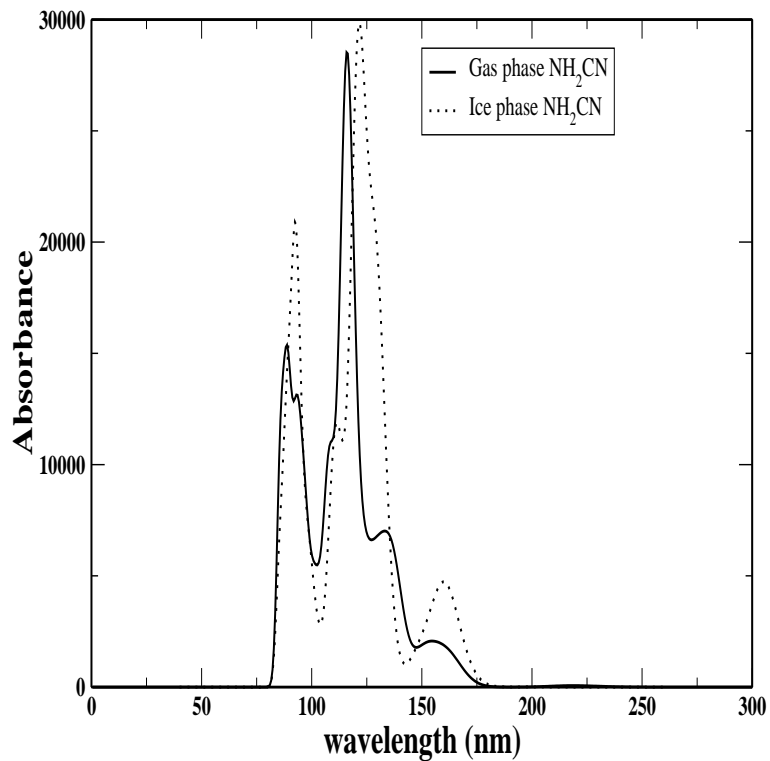


Figure 3: Electronic absorption spectra of NH₂CN in gas as well as in H₂O ice

troscopy to find out the infrared signatures of the vibrational modes of HCCN. They obtained this peak at around 3229 cm^{-1} .

We continue our computation to obtain the spectral properties of HCCN in the electronic absorption mode. However, it does not appear to have any significant contribution. Electronic absorption spectra of NH₂CN molecule in gas (solid) as well in the ice phase (gas) are shown in Fig. 3. The electronic transitions, absorbance and percentage of contribution are summarized in Table 2. An electronic absorption spectrum of NH₂CN molecule in the gas phase is characterized by four intense peaks. These four

Table 2: Electronic transitions of different complex molecules at B3LYP/6-311++G** level theory in gas phase and H₂O ice

Species	Wavelength (gas phase) (in nm)	Absorbance	Oscillator strength	Transitions	Contribution (%)	Wave length (H ₂ O ice) (in nm)	Absorbance	Oscillator strength	Transitions	Contribution (%)
NH ₂ CN	156.2	2058	0.0202	H-0→L+5	38	159.2	4713	0.0837	H-0→L+4	73
	133.7	7003	0	H-1→L+5	86	121.9	10761	0.0002	H-0→L+8	93
	114.83	25998	0.0272	H-2→L+5	81	111.6	11870	0	H-0→L+12	91
	88.9	15378	0.1128	H-3→L+9	72	92.2	20896	0.0168	H-1→L+12	97
CH ₂ NH ₂	397.4	656	0.0162	H-0→L+1	201	365.9	734	0.0176	H-0→L+1	201
	279.6	1560	0.0376	H-0→L+4	199	285.7	2255	0.0548	H-0→L+3	198
	187.6	4774	0.0066	H-0→L+10	103	203.0	2505	0.1055	H-1→L+1	161
	122.0	9633	0.011	H-2→L+2	134	151.0	9357	0.0459	H-1→L+0	166
	104.0	6197	0.0066	H-1→L+12	151	121.2	8975	0.0009	H-1→L+4	195
COOH	262.9	540	0.0120	H-1→L+1	191	259.2	738	0.0174	H-2→L+1	192
	219.2	2777	0.0683	H-0→L+1	194	200.2	1747	0.0363	H-0→L+1	192
	158.4	4349	0.0037	H-2→L+0	120	169.2	6085	0.0936	H-0→L+3	119
	126.4	5938	0.0002	H-3→L+0	122	124.1	11461	0.0162	H-1→L+2	130
	123.2	5887	0.0662	H-0→L+7	149	101.0	6861	0.0086	H-1→L+6	90
	114.4	5581	0.00005	H-2→L+3	86	-	-	-	-	-
101.0	3678	0.0121	H-0→L+10	173	-	-	-	-	-	
C ₂ H ₃ ON	306.8	6245	0.1448	H-0→L+2	93	309.0	8194	0.0108	H-0→L+3	98
	190.0	10132	0.0002	H-0→L+9	88	204.4	4352	0.0063	H-0→L+7	88
	113.0	12982	.0287	H-0→L+20	96	106.3	20307.56	0.0095	H-2→L+9	71
C ₃ H ₃ ON	144.73	6098	0.0317	H-1→L+2	24	-	-	-	-	-
	118.0	19512	0.0178	H-1→L+8	59	118.9	26299	0.0518	H-3→L+5	61

transitions occurred at 156, 133, 114, 89nm with major contributions from H-0→L+4, H-0→L+8, H-0→L+12, H-1→L+12 transitions respectively. Here, H represents the highest occupied molecular orbital (HOMO) and L represents the lowest unoccupied molecular orbital (LUMO). Peaks at 156nm and 89nm are shifted to the right in the ice phase and appear at 159nm and 92nm respectively with a bit high intensities. The peak at 133nm is shifted to 121nm and has a high intensity. The peak at 114nm is shifted to 111nm and has a lower intensity. All the peak locations in electronic absorption spectra with their respective absorbance and oscillator strengths are highlighted in Table 2.

3.2. Precursor molecules of glycine

Observations of glycine are highly debated till date. Several chemical modeling as well as experiments were performed during the past years. Chakrabarti et al. (2000a)

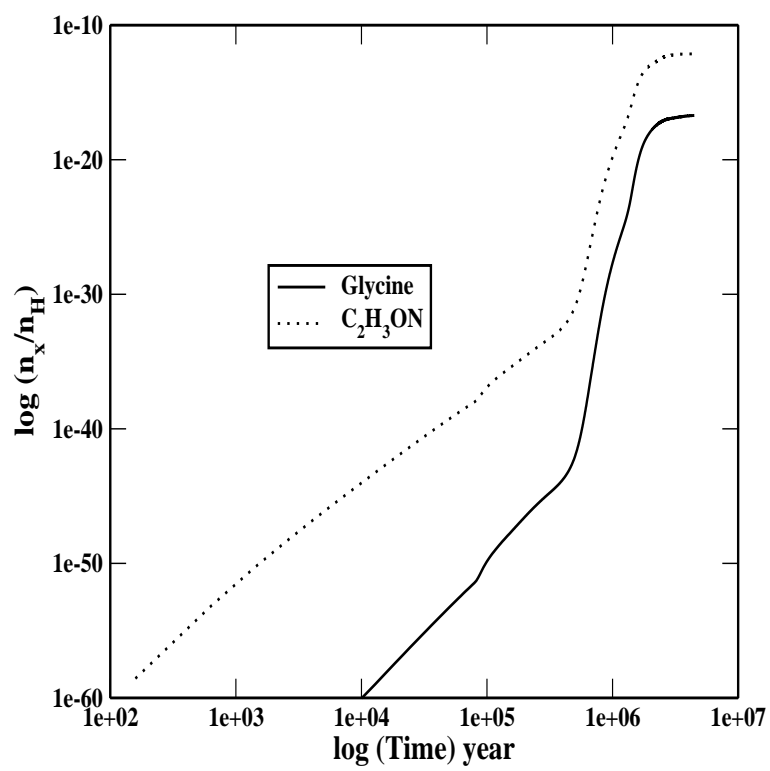
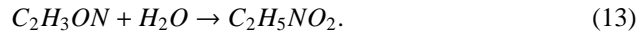


Figure 4: Time evolution of glycine with its precursor molecule, C₂H₃ON. The abundance of the precursor molecule is much higher and could be observed.

proposed the following pathways for the glycine production;

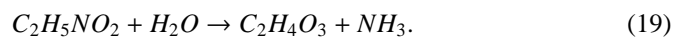


Woon et al., (2002) performed quantum chemical calculations to evaluate the viability of various pathways to the formation of glycine, They considered following pathway:



According to Woon (2002) glycine formation by this method is most likely to happen in such kind of interstellar ices which could have experienced thermal shocks or could have formed in comets that could have passed through warmer regions of the solar system. Since in our model calculations, we are restricted to the temperature 10K, this network does not influence our glycine production at all. So, in our case, glycine is mainly produced by the neutral-neutral pathways, as first discussed by Chakrabarti et al. (2000a). In Fig. 4, the time evolution of glycine along with its precursor

molecule (C_2H_3ON) is shown. Peak abundance of C_2H_3ON and glycine are found to be 7.3×10^{-13} and 1.96×10^{-17} respectively. According to Chakrabarti et al. (2000a) and Majumdar et al. (2012), glycine could react with H_2O to form glycolic acid as the following;



We have included this reaction in our network. Peak abundance of glycolic acid is calculated to be 1.36×10^{-21} . As in Fig. 1, here also a sharp rise in the abundances are observed due to the same reason as discussed in Fig. 1.

Though the pathways proposed by Woon (2002) which does not influence the production of glycine at this low temperature, for the sake of completeness, we have identified CH_2NH_2 and $COOH$ as precursor molecules for the production of glycine by this route. Infrared peak positions with their absorbance in the gas phase as well as in the ice phase is pointed for the species CH_2NH_2 in Table 1. We find that the most intense mode in the gas phase appears nearly at 318 cm^{-1} . This peak is shifted to the right in the ice phase by 77 cm^{-1} and is appearing at 395 cm^{-1} . It is interesting to note that one strong peak appears at 484 cm^{-1} in the ice phase and its corresponding peak in the gas phase spectrum is missing. Several new peaks are significantly pronounced in the ice phase. Similarly, for $COOH$, we have presented similar parameters in Table 1. The gas phase infrared spectrum of $COOH$ mainly consists of three strong peaks. The strongest peak in the gas phase arises at 1719 cm^{-1} (giving an excellent agreement with Chen et al., 1998) followed by two moderate sized peaks at 971 cm^{-1} and 563 cm^{-1} respectively. The strongest peak is shifted to the left in the ice phase and appears at around 1661 cm^{-1} followed by one right shifted peak at around 1004 cm^{-1} and one left shifted

peak at around 527 cm^{-1} respectively. One more prominent peak in the ice phase is pronounced at 2759 cm^{-1} , which is absent in the gas phase. All the ice phase peaks are more intense in comparison to those of the gas phase. Infrared spectral parameters of $\text{C}_2\text{H}_3\text{ON}$ in gas phase as well as in the ice phase are noted in Table 1. We find that gas phase IR spectra of $\text{C}_2\text{H}_3\text{ON}$ contains two major peaks, one at 1133 cm^{-1} and the other at 2127.17 cm^{-1} . From Table 1, it is clear that most of the peaks in gas phase are shifted towards the left for the ice phase spectrum.

Different electronic absorption spectral parameters of CH_2NH_2 in the gas phase and in the ice phase are given in Table 2. In the gas phase, the spectrum is characterized by five intense peaks at 397.4, 279.4, 187.6, 122.0 and 104.0 nm. These intense peaks are assigned due to the $\text{H-0} \rightarrow \text{L+1}$, $\text{H-0} \rightarrow \text{L+4}$, $\text{H-0} \rightarrow \text{L+10}$, $\text{H-2} \rightarrow \text{L+2}$, $\text{H-1} \rightarrow \text{L+12}$ HOMO-LUMO transitions. Peak positions are slightly shifted in the ice phase. In case of COOH also, several intense peaks are prominent in the gas phase at 262.9, 219.2, 158.4, 126.4, 123.2, 114.4 and 101.0 nm. Few of these peaks disappear in the ice phase (Table 2). It is to be noted that most of the peak intensities in the ice phase are considerably higher. Similarly, the electronic absorption spectra of $\text{C}_2\text{H}_3\text{ON}$ in the gas and ice phases are given in Table 2. In the gas phase, it is characterized by three intense peaks at 306.8, 190.0, and 113.0 nm. These intense peaks are assigned due to the $\text{H-0} \rightarrow \text{L+2}$, $\text{H-0} \rightarrow \text{L+9}$, $\text{H-0} \rightarrow \text{L+20}$ HOMO-LUMO transitions. These peak positions are slightly shifted in the ice phase.

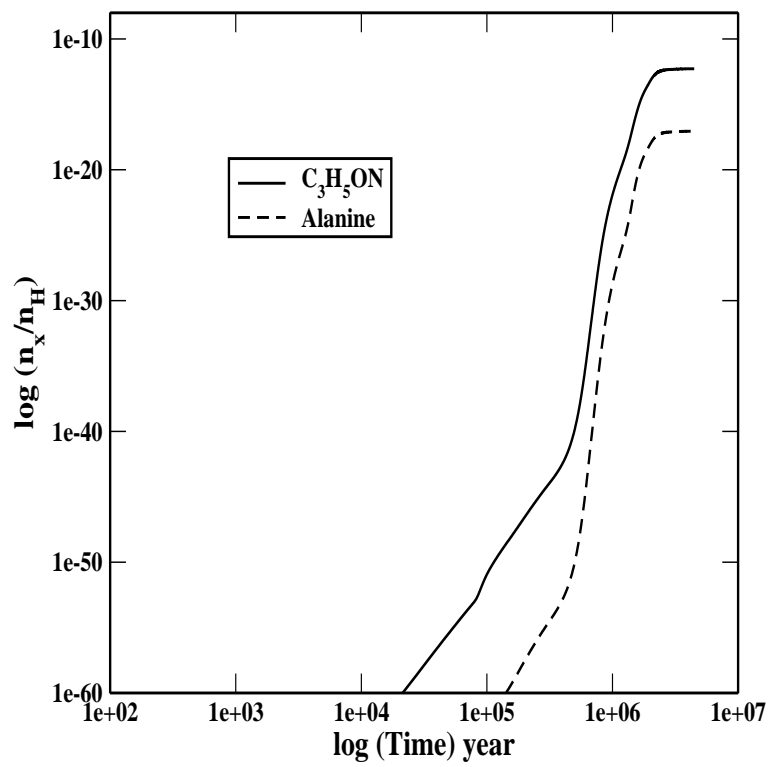


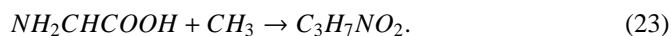
Figure 5: Time evolution of alanine with its precursor molecule, $\text{C}_3\text{H}_5\text{ON}$.

3.3. Precursor molecules of alanine

According to Chakrabarti et al., 2000a, the alanine formation could be due to the following reactions:



According to Woon et al., (2002) production could follow the following route;



Woon et al., (2002) discussed the production of Alanine in the UV irradiated ice, which are much warmer. So this pathway is not relevant in the present situation. So the neutral-neutral pathways as described by Chakrabarti et al. (2000a) could be very useful. In the neutral-neutral reaction pathway, C_3H_5ON reacts with highly abundant gas phase H_2O to form alanine. Similar to the chemical evolution of adenine and glycine shown in Fig. 1 & Fig. 4 respectively, chemical evolution of this precursor molecule along with the alanine is shown in Fig. 5. Hydro-chemical modeling suggests that C_3H_5ON having a peak abundance of 5.3×10^{-13} could produce alanine with a peak abundance of 8.9×10^{-18} . Here too, the precursors are several orders of magnitude more abundant and they would be more easily detectable.

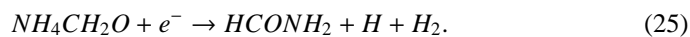
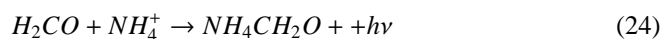
Infrared peak positions along with the absorbance of C_3H_5ON in the gas as well as in the ice phase are highlighted in Table 1. The gas phase spectrum consists of several

intense peaks. There are two strong peaks located at 290 cm^{-1} and 1033 cm^{-1} respectively. In the ice phase, several new peaks appear which have much higher intensity. The strongest peaks in the ice phase appear at 3243 cm^{-1} , 278 cm^{-1} and 263 cm^{-1} respectively. All other peak locations are given in Table 1.

The electronic absorption spectrum of $\text{C}_3\text{H}_5\text{ON}$ molecule in gas phase is characterized by two intense peaks arising due to the $\text{H-1} \rightarrow \text{L+2}$, $\text{H-1} \rightarrow \text{L+8}$ HOMO-LUMO transitions. The ice phase electronic absorption spectrum is followed by only one peak (Table 2) at the wavelength 118.9 nm . The peak positions along with all the details of the electronic absorption spectra are given in Table 2.

3.4. Formamide: An important precursor in the abiotic synthesis of amino acids

Formamide is the simplest amide containing peptide bond. It is very abundant in the ISM and could be an important precursor in the abiotic synthesis of amino acids and thus significant to further prebiotic chemistry in the interstellar space. Formamide was discovered in the interstellar space in the early 1970s. It has been identified by one of the gas phase molecules in the past (Millar, 2004). It is also highly abundant in the ice phase (Garrod et al., 2008). Formamide in the ISM could be produced by several pathways. Here we have mainly followed Quan & Herbst (2007) for its production in the gas phase.



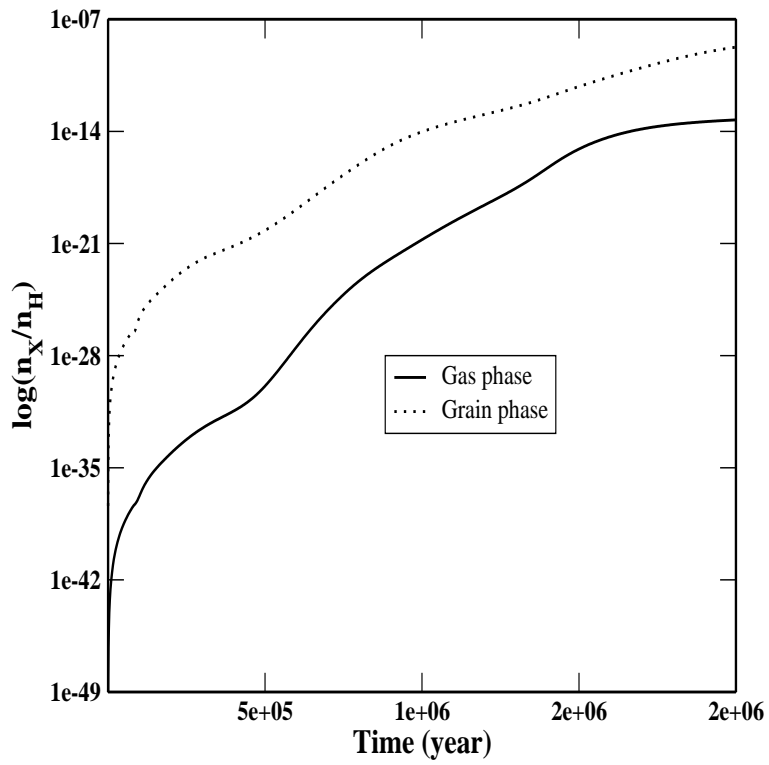
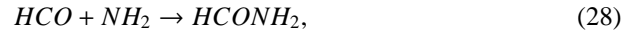
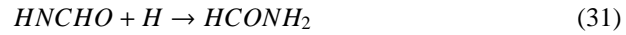
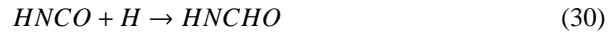


Figure 6: Time evolution of formamide in the gas phase as well as in the ice phase.

For the production of Formamide in the ice phase we follow Jones et al., (2011) who suggested the pathway below:



and Garrod et al., (2008) who suggested the pathway as given below:



Since reaction number 28 could also be possible in the gas phase, we include this reaction in our gas phase network as well. Following the same technique used in Majumdar et al., (2012), the reaction energy for this reaction is calculated to be -4.12 eV and the rate coefficient calculated to be $2.73 \times 10^{-11} \text{ cm}^3 \text{ S}^{-1}$. In Fig. 6, we have shown the time evolution of the formamide in the gas phase as well as in the ice phase. The peak abundance of the gas phase formamide is calculated to be 1.33×10^{-13} , whereas the grain phase formamide appears to be highly abundant (9.45×10^{-9}).

Recently Sivaraman et al. (2012), performed an experiment to obtain the IR spectra of the formamide in the ice phase. They used experimental setup based at The

Table 3: Vibrational frequencies of Formamide in gas phase, H₂O ice and methanol containing grains at B3LYP/6-311G++** level of theory

Species	Peak positions (Gas phase) (Wavenumber in cm ⁻¹)	Absorbance	Peak positions (H ₂ O ice) (Wavenumber in cm ⁻¹)	Absorbance	Peak positions (Methanol ice) (Wavenumber in cm ⁻¹)	Absorbance	Peak position (Mixed ice) (Wavenumber in cm ⁻¹)	Absorbance	Peak positions by Experiment (Wavenumber in cm ⁻¹)
H₂NCHO	535.27	217.71	574.75	24.36	574.72	23.96	574.72	24.34	-
	566.2	11.04	600.39	202.88	598.11	297.18	598.25	305.54	-
	656.9	134.94	668.7	202.88	669.25	200.41	670.22	198.46	-
	1035.82	2.7188	1053.77	5.21	1053.25	5.2	1055.15	5.18	1022
	1067.82	3.46	1082.36	2.24	1082.29	2	1083.01	2.16	1056
	-	-	-	-	-	-	-	-	1117
	-	-	-	-	-	-	-	-	1172
	1280.07	115.04	1309.74	134.26	1308.97	135.88	1309.8	134.71	1226
	-	-	-	-	-	-	-	-	1334
	1416.33	27.68	1387.4	168.36	1388.86	158.32	1388.84	167.9	1386
	1654.2	44.98	1602.01	311.72	1604.49	300.78	1603.19	293.25	1628
	1697.36	405.23	1641.11	504.78	1643.25	503.21	1640.75	523.72	1698
	3000.13	88.48	2996.46	32.04	2997.12	33.95	2991.10	32.51	2895
	-	-	-	-	-	-	-	-	3179
	3569.63	27.22	3398.15	183.5	3405.10	175.06	3396.87	182.07	3372
	3715.58	27.94	3528.69	156.17	3536.57	149.65	3529.07	157.64	-

Open University, UK (Sivaraman et al., 2008) to simulate astrochemical ices and their irradiation environments. The instrument was operated at base pressure of the order of 10^{-10} Torr, and it could go down up to the temperature 28K. Low temperature was achieved by using a closed cycle helium cryostat. A CaF₂ substrate was placed at the end of the cryostat onto which the molecular gases were directly deposited to form multilayer targets. Sample temperature measurements were carried out using a silicon (Si) diode sensor calibrated using the calibration curve provided by the Scientific Instruments. Formamide samples 99.5 % pure (from Sigma Aldrich), were used. Before introducing the formamide vapour into the chamber, the liquid sample was processed by three freeze-pump-thaw cycles to degas any absorbed impurities. The sample was then allowed to return to room temperature before extracting the vapours to form the ice on the CaF₂ substrate.

We compare our theoretical result with this recent experiment. Figure 7 shows the normalized infrared spectra of formamide molecule in the ice phase (where H₂O was used as a solvent) which we calculate along with the experimentally obtained infrared

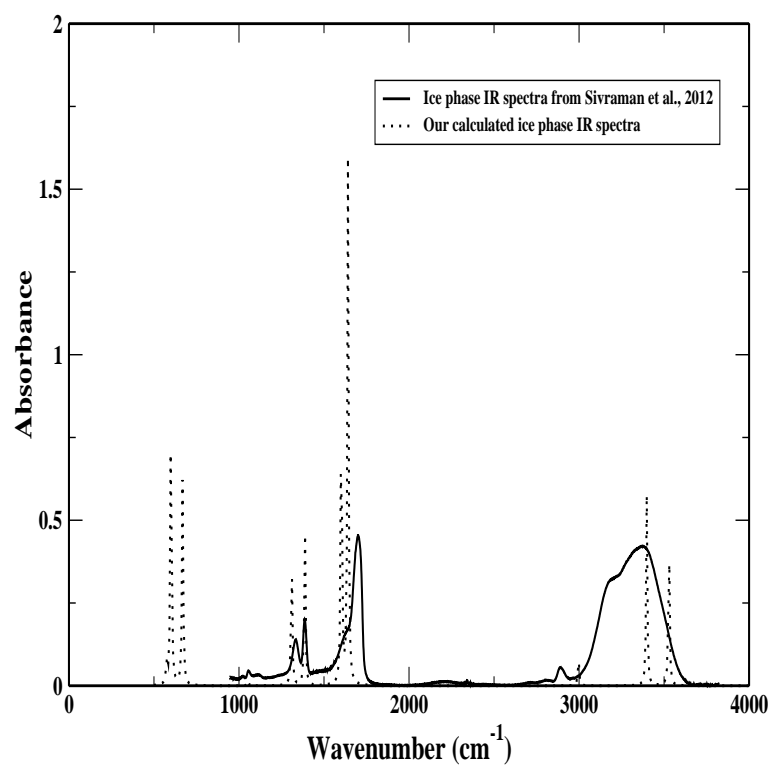


Figure 7: Comparison between the ice phase formamide IR spectra obtained by our quantum chemical approach and experimental approach by Sivaraman et al., 2012

spectra of formamide at 30K before irradiation. Peak positions are given in Table 3. It is clear from Table 3 that some of the calculated peaks are very close to the experimental values. For example, our calculated peak position is at 1387.40 cm^{-1} , whereas the experimentally obtained peak location is at 1386 cm^{-1} . Beside this, there are a few more peaks which are close to the experimental values (Table 3). **To have an idea about the effect of solvent upon the spectrum, we considered different kind of ice as a solvent. In general, we have considered the water ice but depending upon the properties around the molecular cloud, ice composition may be different (Das et al., 2010). Keeping this, first we consider pure methanol ice instead of pure water ice and study the changes in the peak positions and intensities (Table 3). Second, based on the observational results, we consider a mixed ice, which consists of 70% water, 20% methanol and 10% CO_2 molecules and noted down the spectral properties in Table 3. From Table 3, it is evident that the peak positions of formamide in methanol containing ice and mixed ice are slightly shifted in compare to the formamide in pure water ice.** Though some peak positions are closely coinciding with our theoretical calculations, some observed peaks are well above our values. Our quantum chemical calculations are based upon the Ab initio methods in GAUSSIAN 09, which employ the Born-Openheimer approximation in generating the energy expressions. It then allows us to separate the nuclear and electronic degrees of freedom. The energy is the electronic energy parameterized by the frozen locations of the nuclei and because they are frozen, the model simulates at 0K, whereas the experiment was performed at 30K. Moreover, here we are not considering the clusters of formamide for calculating the spectra. Rather, we are including one formamide molecule in a

Table 4: Electronic transitions of Formamide at B3LYP/6-311++G** level theory in gas phase and H₂O ice

Species	Wavelength (gas phase) (in nm)	Absorbance	Oscillator strength	Transitions	Contribution (%)	Wave length (H ₂ O ice) (in nm)	Absorbance	Oscillator strength	Transitions	Contribution (%)
H₂NCHO	184.8	3365	0.0736	H-0 → L+2	99	166.7	17903	0.189	H-0 → L+2	43
	163.4	13685	0.3215	H-1 → L+1	65	114.5	12348	0.088	H-3 → L+1	56
	122.5	5963	0.0122	H-3 → L+0	98	92.2	13377	0.0236	H-0 → L+16	93
	115.5	5647	0.0531	H-2 → L+1	33	-	-	-	-	-
	100.1	11453	0.1258	H-3 → L+5	55	-	-	-	-	-
	92.0	11963	0.0326	H-0 → L+16	92	-	-	-	-	-

spherical cavity, which is immersed in a continuous medium with a dielectric constant.

Here the solute-solvent electrostatic interactions are treated at the dipole level. The solvent effect brings significant changes in the geometrical parameters of formamide. Our model confirms that the polarization of the solute by the continuum has important effects on the absolute and relative solvation energies, which, in turn, shift the frequency and vary the intensity in the infrared mode. On the other hand, during the experiment, several clusters could be formed. So, an ideal match is not expected.

Electronic absorption spectral parameters of formamide molecule in gas phase as well as in the ice phase are highlighted in Table 4. An electronic absorption spectrum of formamide molecule in gas phase is characterized by 3 intense peaks. These three transitions occurred at 163.4, 100.1, 92.0 nm with major contributions from H-1 → L+1, H-3 → L+5, H-0 → L+16 transitions respectively. With these strong peaks, some substructures are also prominent in the gas phase, which are completely absent in the ice phase. As in the other cases, these intense peaks are due to the transition from HOMO to LUMO (Table 4).

4. Conclusion

In this paper, we have explored the infrared and electronic absorption spectra of various complex molecules, which could be treated as the precursors of adenine, glycine and alanine in several astronomical situations. **Since we use a realistic scenario with hydro-chemical evolutions with accurate rate coefficients (Majumdar et al. 2012) our results could be significant for future observations.**

In comparison with the gas phase spectra, the spectral properties in the ice phase are significantly different. Various peak positions are shifted and some peaks completely disappeared. Some substructures became pronounced also in the ice phase. **Based on the observational results, we simulated our grain mantle differently which have different ice compositions. We considered the ice to be that of pure water or pure Methanol or even mixed (70% water 20% methanol and 10% CO₂) in nature. We have highlighted the dependence of the spectral changes on the solvent types**

We computed the chemical evolution of adenine, alanine & glycine along with their precursor molecules. We pointed out that the computed abundances of the precursor molecules are within the observational limits and could be detected in future. Based on the abundances of these precursor molecules, one could estimate the abundances of the molecules of our interest. We made a comparison between our calculated infrared spectra of formamide and experimentally obtained infrared spectra. Some of the peak locations are found to coincide while a few others do not match. We presented possible reasons behind this.

There are ample debates on whether alanine, glycine or adenine has been seen in interstellar medium or not, It is possible that the abundances of these molecules are very

small and the present day equipments lack sufficient sensitivities. However, our paper probes the feasibility of observing the precursors of these very important molecules and computed abundances seem to indicate that they are observable, in principle. We have also computed the spectral features, i.e., the wavelengths where the characteristic peaks would be observed. We anticipate that these results would be appreciated by observers.

5. Acknowledgment

We acknowledge the help of Dr. B. Sivaraman, INSPIRE Faculty (IFA-11CH -11), Indian Institute of Science, B. N. Raja Sekhar of AMPD, BARC at RRCAT Indore and N. J. Mason of The Open University for supplying us with the experimental IR data for Formamide. LM, SKC & SC are grateful to DST for the nancial support through a project (Grant No. SR/S2/HEP-40/2008) and AD thanks ISRO respond project (Grant No. ISRO/RES/2/372/11-12).

References

- [1] Abelson, P. H., 1966, Proc. Natl. Acad. Sci., 55, 1365
- [2] Bates, D. R., 1983, ApJ 270, 564
- [3] Bujarrabal, V., Fuente, A., Omont, A., 1994, A&A, 285, 247
- [4] Chakrabarti, S.K., Das, A., Acharyya, K., Chakrabarti, S., 2006, A&A, 457, 167
- [5] Chakrabarti, S.K., Das, A., Acharyya, K., Chakrabarti, S., 2006, BASI, 34, 299

- [6] Chen, J., Hamon, M. A., Yongsheng Chen, H. H., Rao, A. M., Eklund, P. C., Had-
don, R. C., 1998, *Science*, 282, 95
- [7] Cuppen, H. M., Herbst, E., 2007, *APJ*, 668, 294
- [8] Cuppen, H. M., Van Dishoeck E., F., Herbst, E., Tielens, A. G. G. M., 2009, *A&A*,
508, 275
- [9] Das, A., Chakrabarti, S. K., Acharyya K. & Chakrabarti, S., 2008a, *NEWA*, 13,
457
- [10] Das, A., Acharyya, K., Chakrabarti, S. & Chakrabarti, S. K., 2008b, *A & A*, 486,
209
- [11] Das, A., Acharyya, K. & Chakrabarti, S. K., 2010, *MNRAS* 409, 789
- [12] Das, A. & Chakrabarti, S. K., 2011, 418. 545, *MNRAS*
- [13] Das, A. Majumdar, L., Chakrabarti, S. K., & Chakrabarti S., 2012, *NEWA* (sub-
mitted)
- [14] Dendramis, A., Leroi, G. E., 1977, *JCP*, 66, 4334
- [15] Draine, B. T., 2003, *ApJ* 598, 1017
- [16] Garrod, T, Weaver, S. L. W., Herbst, E., 2008, *APJ*, 682,283
- [17] Gibb, E. L., Whittet, D. C. B., Boogert, A. C. A., & Tielens, A. G. G. M. 2004,
ApJS, 151, 35
- [18] Gupta, V.R., Tandon, P., Rawat, P., Singh, R.N. & Singh, A., *A&A*, 528, A129

- [19] Guelin, M., & Cemicharo, J. 1991, A&A, 244, L21
- [20] Hasegawa, T., Herbst, E., Leung, C.M., 1992, APJ, 82, 167
- [21] Hollis, J.M. et al., 2003, ApJ 588, 353
- [22] Jiurys, L. M. 2006, Proc. Nat. Acad. Sci., 103, 12274
- [23] Jones, B. M., Bennett, C., Kaiser, R., 2011, APJ, 734, 78
- [24] Keane, J. V., Boogert, A. C. A., Tielens, A. G. G. M., Ehrenfreund, P., Schutte, W. A., 2001, A&A, 375L, 43
- [25] Kuan, Y.J., Charnley, S.B., Huang, H.C., Tseng, W.L., Kisiel, Z., 2003. ApJ 593, 848.
- [26] Liszt, H., & Lucas, R. 2001, A&A, 370, 1
- [27] Majumdar, L., Das, A., Chakrabarti, S.K., Chakrabarti, S., 2012, RAA (accepted)
- [28] McCarthy, M. C., Gottlieb, C. A., Coosky, A. L., Thasseus, P., 1995, JCP, 103, 7779
- [29] McGonagale, D., Irvine, W. M., 1996, A&A, 310, 970
- [30] Millar, T.J. 2004, Organic molecules in the interstellar medium. In *Astrobiology: future perspectives*, Kluwer Academic Publisher vol. 305, 17
- [31] Orgel, L. E., 2004, Biochem Mol. Biol., 39, 99
- [32] Omont, A., 1993, J. Chem. Soc. Faraday Trans, 89, 2137

- [33] Rubalcava, Hector, 1956, Ph.D. thesis, California Institute of Technology.
<http://resolver.caltech.edu/CaltechETD:etd-06242004-155629>
- [34] Sivaraman, B., Ptasinska, S., Jheeta, S., Mason, N.J., 2008. Chem. Phys. Lett.
460 (1-3),108
- [35] Sivaraman, B., Raja Sekhar B. N., Nair, B. G., Hatode, V., Mason, N. J.,2012,
Spectrochimica Acta: part A-molecular and biomolecular spectroscopy (submitted)
- [36] Quan, D., Herbst, E., 2007, A&A, 474, 521
- [37] Snyder, L.E. et al., 2005,. ApJ 619, 914.
- [38] Turner, V. E., List, H. S., Kaifu, N., & Kisliakov, A. G. 1975, ApJ, 201, L149
- [39] Woodall, J., Agnèz, M., Markwick-Kemper, A.J., Millar, T.J., 2007, A&A, 466,
1197
- [40] Woon, D.E., 2002, APJ, 571, L177